

DEPARTMENT OF ENERGY, MINES AND RESOURCES
OTTAWA

QC

151

B6

1970

THE CHANGE OF WATER LEVEL
CAUSED BY THE VARIATION OF THE
INFLOW-OUTFLOW ON LAKE ONTARIO

BY PAUL-ANDRE BOLDUC

OTTAWA, MARCH 1970

TABLE OF CONTENTS

	LIST OF CAPTIONS	
I	INTRODUCTION	1
II	THEORY	1
III	NUMERICAL METHOD	4
IV	ANALYSIS OF THE MODEL	6
	A: SIMPLIFIED MODEL	6
	B: REAL MODEL	8
V	CONCLUSION	11
	ACKNOWLEDGEMENT	12
	REFERENCES	13

LIST OF CAPTIONS

FIGURE 1	Coordinates used in the Basic Equations	15
FIGURE 2	Arrangements of the Grid Points for Consecutive Time Steps in the Numerical Solution	15
FIGURE 3	Simplified Rectangular Model	16
FIGURE 4	Real Numerical Model of Lake Ontario	17
FIGURE 5	Chezy's Coefficient " C "	18
FIGURE 6	Smoothing Coefficient " α "	18
FIGURE 7	Time Step " Δt "	19
FIGURE 8	Inflow-Outflow of the Lake " Q "	19
FIGURE 9	Comparison between the Simplified and the Real Model	20
FIGURE 10	Response of the Model to the Input Sine Function	21
FIGURE 11	Response of the Model to the Output Sine Function	22
FIGURE 12	Calculated Water Level with Sine Function Applied to the Niagara	23
FIGURE 13	Calculated Water Level with Sine Function Applied to the St. Lawrence	24
FIGURE 14	Amplitude of the Sine Wave for Particular Points in Lake Ontario, Sine Function Applied to the Niagara	25
TABLE 1	Discharge Values used in the Model	26
TABLE 2	Amplitude of the Sine Wave	27

INTRODUCTION

Many of us assume that the water surface of a lake is a true level surface because the water always tends to seek the equilibrium. Surveyors sometimes use such level surfaces in establishing elevations, thus saving time and effort while trying to maintain the usual accuracy of instrumental level loops. It has been mentioned however by several investigators that a lake surface is not level since natural oscillations caused by wind tides, wind set-up, variation of discharge, difference of water temperature and different density may tilt the lake surface permanently or over a prolonged period of time.

Each of these causes have their particular effects on the water level variation while an observer sees only the total change. Our purpose is to study these causes separately and to evaluate the influence each of them has on the water surface.

This first report is an analysis on the variation of the water level of Lake Ontario caused by the relation of the inflow of the Niagara River and the outflow through the St. Lawrence River.

THEORY

Dronkers (1964) shows that in a two-dimensional model as shown in Figure 1, the equations of motion for long waves in a horizontal plane in a large body of water are:

$$\begin{aligned} \frac{\partial u}{\partial t} + u \frac{\partial u}{\partial x} - v \frac{\partial u}{\partial y} - f v = \\ -g \frac{\partial h}{\partial x} - \frac{1}{\rho_0} \frac{\partial P^a}{\partial x} + T_x^w - T_x^b \end{aligned} \quad (1)$$

$$\begin{aligned} \frac{\partial v}{\partial t} + u \frac{\partial v}{\partial x} + v \frac{\partial v}{\partial y} + f u = \\ -g \frac{\partial h}{\partial y} - \frac{1}{\rho_0} \frac{\partial P^a}{\partial y} + T_y^w - T_y^b \end{aligned} \quad (2)$$

where u = velocity of the flow in the x direction

v = velocity of the flow in the y direction

t = time

f = Coriolis parameter

g = gravitational force of the earth

h = height above the mean water level

P^a = atmospheric pressure

ρ_0 = air density

T_x^b = bottom stress in the x direction

T_y^b = bottom stress in the y direction

In these two equations, the corrective terms

$(u \frac{\partial u}{\partial x} + v \frac{\partial u}{\partial y}; u \frac{\partial v}{\partial x} + v \frac{\partial v}{\partial y})$ can be neglected because of their small

amplitude. The influence of the wind and the variation in the

atmospheric pressure $(T_x^w, \frac{-1}{\rho_0} \frac{\partial P^a}{\partial x}; T_y^w, \frac{-1}{\rho_0} \frac{\partial P^a}{\partial y})$ are neglected in

this paper. The equations (1) and (2) can then be rewritten in

a simplified form:

$$\frac{\partial u}{\partial t} - f v = -g \frac{\partial h}{\partial x} - T_x^b \quad (3)$$

$$\frac{\partial v}{\partial t} + f u = -g \frac{\partial h}{\partial y} - T_y^b \quad (4)$$

The Coriolis parameter can be expressed as

$$f = 2 w \sin \Psi \quad (5)$$

where w = angular velocity of the earth

Ψ = latitude of the area

Dronkers (1964) shows that the bottom stress T_x^b and T_y^b are expressed as follows:

$$T_x^b = \frac{g}{C^2 (a_o + h)} |V| u \quad (6)$$

$$T_y^b = \frac{g}{C^2 (a_o + h)} |V| v \quad (7)$$

where C = De Chezy's coefficient

$$V = \sqrt{u^2 + v^2}$$

a_o = mean depth

To solve this set of equations (3 and 4), we need another relation between the velocity components and the elevation of water. This function is given by the continuity equation and can be expressed as:

$$\frac{\partial h}{\partial t} + (a_0 + h) \frac{\partial u}{\partial x} + (a_0 + h) \frac{\partial v}{\partial y} = 0 \quad (8)$$

Equations (3), (4) and (8) represent completely the motion of water in the time and space domain and have to be solved simultaneously.

NUMERICAL METHOD

The analytical solution of these three differential equations is impossible. Several methods have been developed to overcome this difficulty. One might use a representation of the phenomenon by a suitable continuous function, as for example a truncated Fourier series. But, as stated by Welander (1961), as most numerical prediction experiments made in the past have been based on a step-by-step integration, finite difference methods have been used in this work. As central differences are exact to a higher order in " Δt " than the forward difference and since such a solution is more stable than the forward difference, we prefer to use central difference in the time direction.

In order to solve the differential equations numerically, they have to be broken down so that the independant variables are represented by discrete numbers. If m , n and k represents respectively the integer increment in the x , y and t as shown in Figure 2, we can write equations (3), (4) and (8) as follows:

$$U_{m,n}^{k+1} = U_{m,n}^{k-1} + 2\Delta t f V_{m,n}^k - \frac{\Delta t q}{\Delta x} \left[H_{m+1,n}^k - H_{m-1,n}^k \right] - 2\Delta t \left[T_x^b{}^k{}_{m,n} \right] \quad (9)$$

$$V_{m,n}^{k+1} = V_{m,n}^{k-1} - 2\Delta t f U_{m,n}^k - \frac{\Delta t q}{\Delta y} \left[H_{m,n+1}^k - H_{m,n-1}^k \right] - 2\Delta t \left[T_y^b{}^k{}_{m,n} \right] \quad (10)$$

$$H_{m,n}^{k+1} = H_{m,n}^{k-1} - \frac{\Delta t}{\Delta x} \left[A_{om,n} + H_{m,n}^k \right] \left[U_{m+1,n}^k - U_{m-1,n}^k \right] - \frac{\Delta t}{\Delta y} \left[A_{om,n} + H_{m,n}^k \right] \left[V_{m,n+1}^k - V_{m,n-1}^k \right] \quad (11)$$

In order to compute the values of U , V , and H at time $(k+1)$ we need to know the values at time (k) and at time $(k-1)$. At the beginning of the calculation process we apply the boundary conditions at time (1) , while all the values at time (0) and (-1) are set to zero. It takes at least three iterations in the time domain before the results come to significant figures.

Numerical methods being an approximation of the real solution, errors can be expected if nothing is done to control them. Platzman (1953) shows that to obtain numerical stability, the following conditions have to be fulfilled:

$$\sqrt{2gh} \Delta t / \Delta s < 1 \quad (12)$$

For safety practice it is recommended to use such small time-steps that the above condition is well below one. Unstability arises too with repetitive numerical errors introduced in the calculation because of the generation of noise in the model.

Welandar (1961) suggests using a smoothing operator:

$$As_{m,n}^k = \alpha A_{m,n}^k + \frac{1-\alpha}{4} \left[A_{m+1,n}^k + A_{m-1,n}^k + A_{m,n+1}^k + A_{m,n-1}^k \right] \quad (13)$$

where As is the smoothed value and α is a constant, $0 < \alpha < 1$. This smoothing operator is very useful when numerical instability is introduced by the non-linearity in the differential equations.

ANALYSIS OF THE MODEL

A: Simplified Model

A simplified rectangular model as shown in Figure 3 of uniform depth equals to 61 meters was first used to test the equations (9), (10) and (11) on the computer. The width and length are equal to 89 and 283 kilometers respectively. A value of 17.7 kilometers was used for Δy and Δx . The mesh system was established to have a "U" and "V" calculation at the outlet of the Niagara River ($M=4, N=1$) and at the entrance of the St. Lawrence River ($M=15, N=6$ and $M=17, N=6$). It should be noted that an "H" is calculated only at every second space step as shown in Figure 2. The grid system remains the same at every time step of the calculation. The boundary conditions applied to the model are the discharge of the Niagara and the St. Lawrence Rivers.

In the first trial, the discharge was assumed to be a step function applied at both the inlet and the outlet of the model. Depending on the values used for the parameters in the model, the steady state condition was reached at different times. Figures 5 to 8 show

the variation of this time with respect to Chezy's coefficient "C", the smoothing coefficient " α ", the time-step " Δt " as used in the calculation and the magnitude of the discharge " Q ". The time to steady state was determined when there was no change (or less than five percent) in the computed values. As there are fifty-one "H" points in the model, we determined the mean, the maximum and the minimum time to steady state. This first analysis gave us the following information:

- a) the variation of Chezy's coefficient is not significant because of the depth of the lake used in the calculation.
- b) the smoothing coefficient " α " is critical for value higher than 0.90, meaning if no smoothing is used, noise is generated in the model and the steady state is never reached. We found out that a value for α of 0.85 gave good results.
- c) the time step must be chosen very carefully and furthermore a big time step does not necessarily save calculation time as the total running time has to be increased quite considerably to reach the steady state. Even with the same value of Δy and Δx the numerical stability is reduced only if the condition stated by equation (12) is verified.
- d) the magnitude of the discharge does not affect appreciatively the mean value of the time to steady state.

B: Real Model

Specifying the Chezy's coefficient " C " equals to $30.4 \text{ m}^{\frac{1}{2}}\text{-sec}^{-1}$, the smoothing coefficient " α " to 0.85, the time step " Δt " equals to 2 minutes, the same step function of magnitude equals to $8858 \text{ m}^3\text{-sec}^{-1}$ was run on the real and the simplified model.

Comparison between the two models cannot be made easily because they react quite differently to the same step input function. Figure 9 illustrates the difference between the response of the two models for five selected points corresponding to the coordinates of the gauging stations. The simplified model illustrates only the tendency and the shape of the response curve while the values of elevation differ appreciably. It clearly shows that too much simplification cannot be made and that the elevation of the points and the general shape of the lake must be as close as possible to reality.

Then the model is tested by simulating a sinusoidal variation of discharge at one inlet while the other is kept constant. This flow condition can be represented as:

$$Q'_1 = \text{constant} \quad (14)$$

$$Q'_2 = Q_0 + Q_1 \sin wt \quad (15)$$

The time has to be expressed in seconds and w is taken as the fundamental frequency of Lake Ontario as stated by Rockwell (1966) being one cycle every 4.8 hours.

The magnitude of Q_0 , Q_1 and Q_{CTE} as shown in Table 1 was established by analysing the 1968 data available, meaning the hourly mean discharge for the Niagara River and the daily mean discharge for the St. Lawrence River. These values were chosen so that the sine function represents the greatest variation in the discharge function, thus simulating the river flow during the winter months. Figures 10 and 11 show the response of five selected points when the first and the second conditions are applied respectively. The bottom stress is neglected in this part of the study.

The response of the model is more pronounced on the points surrounding the inlet than to those surrounding the outlet. This is due to the fact that the cross section area of the St. Lawrence is so big that the computed flow ($V = Q/A$) becomes too small. The figures show too that the period of the sine wave is conserved and that the amplitude remains the same during all the calculation time. The absence of the damping effect in the model is also noticeable. To observe the damping effect, one has to introduce the bottom stress into the calculation procedure. This has been done, but as Chezy's coefficient is not significant as stated earlier, only the third significant digit changed when the bottom stress is applied. Figures 10 and 11 show that there is a considerable difference in the amplitude from point to point and that the phase difference is also very significant. Figure 11 illustrates that the convergence time differs for the calculated points.

Figures 12 and 13 give the water level for fifty-one "H" points at time 740 minutes after the start of the calculation. The water level varies from point to point because each one reacts differently to the applied functions. It shows that the lake is tilting, with other words that one end of the lake is at a higher elevation than the other. We can notice too that there is no correspondence between an (n) and an $(n+1)$ line. For example, this results in the following pattern:

$n+2$	72		44
$n+1$		-1	
n	450		204
	m	$m+1$	$m+2$

The (-1) value looks suspicious among the other values. This is caused by the calculation process because the grid system is not refined enough. A smoothing technique should be used to reduce this effect of computation.

Table 2 shows the maximum, the mean and the amplitude of the sine wave for various points. Figure 14 illustrates the amplitude of the sine wave for different locations on the lake. As it is expected, the amplitude is decreasing with the distance from the inlet of the lake. We can see that the amplitude is decreasing from

130 to 102 millimeters when the distance increases in the x direction to station 52 and it decreases from 382 to 30 millimeters in the y direction to station 53. The difference between 130 and 382 millimeters for two points with the same distance from the inlet is caused by the direction of the flow. Most of the flow is moving in the positive y direction while only a small part is moving in the negative x direction.

CONCLUSION

With this numerical model we have been successful in analysing the change of water level caused by the relation of the inflow-outflow on Lake Ontario. We plan to study the other causes of variation such as wind and atmospheric pressure with the same model. Before doing so, we think that we should analyse the effect of changing the value of the space step. Will a more refined grid system give better results? This will have to be analysed with the real model because the influence of the shape of the lake is not negligible. Work will be carried out on the combined effects of all the causes of variation. On shore meteorological data will be required as input in the model. Several stations will be installed this summer around the lake for this purpose. Then it will be possible to compare the results with the water level data available on Lake Ontario and make appropriate corrections to bring the water level to a levelling surface.

ACKNOWLEDGEMENT

The author wishes to acknowledge his gratitude to Mr. G. C. Dohler and Mr. L. F. Ku for their support and worthwhile discussions.

Thanks are also due to all the members of the Tidal Services and especially to Miss S. Ostapyk for the typing work.

REFERENCES

Dronkers, J. J., 1964. Tidal Computations in Rivers and Coastal Waters. John-Wiley & Sons.

Welanders, P., 1961. Numerical Prediction of Storm Surges. Advances in Geophysics, Volume 8, Academic Press, New York & London.

Platzman, G. W., 1958. A numerical Computation of the Surge of 26 June 1954 on Lake Michigan. Geophysics, 6, pp 407-438.

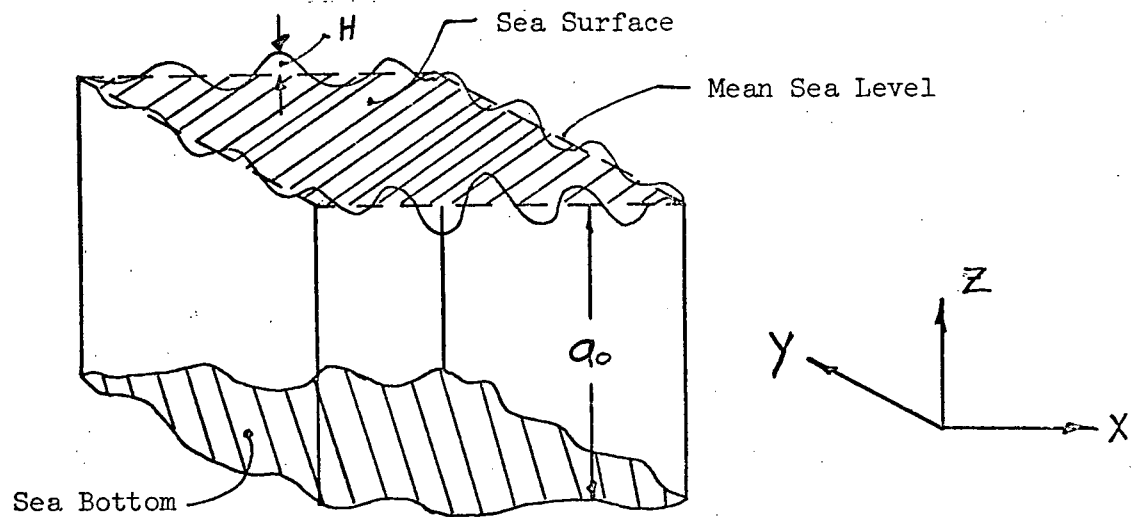
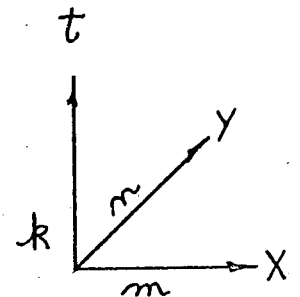
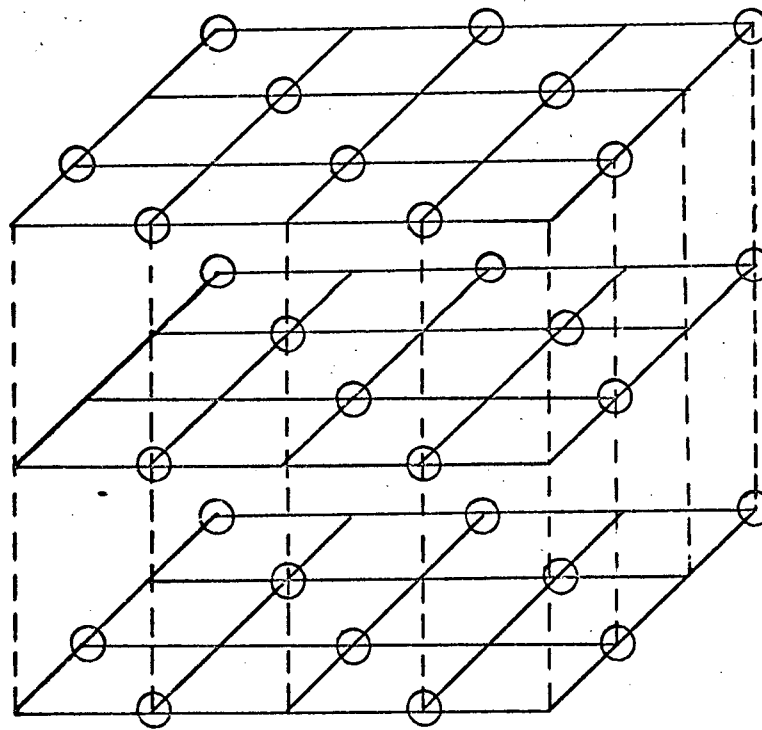


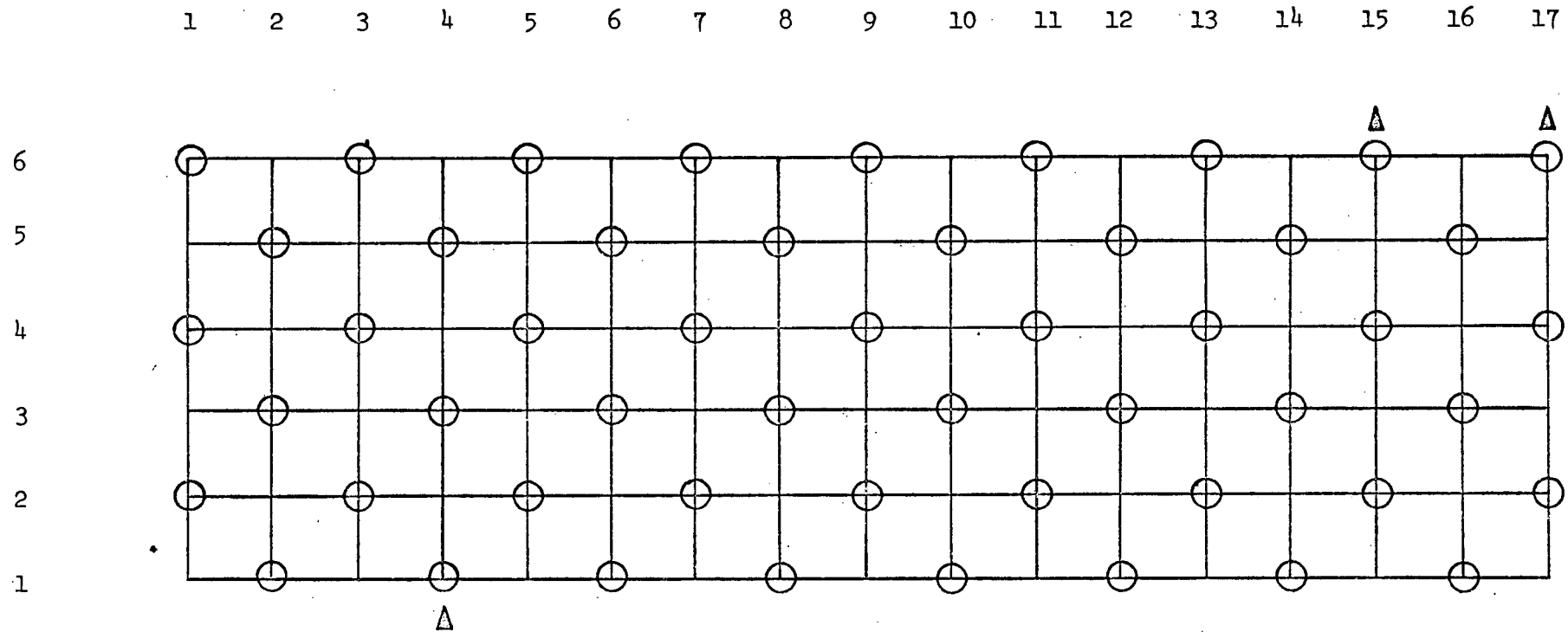
Figure 1 Coordinates Used in the Basic Equations






+ H calculation

⊗ U & V calculation

Figure 2 Arrangements of the
Grid Points for Consecutive Time
Steps in the Numerical Solution

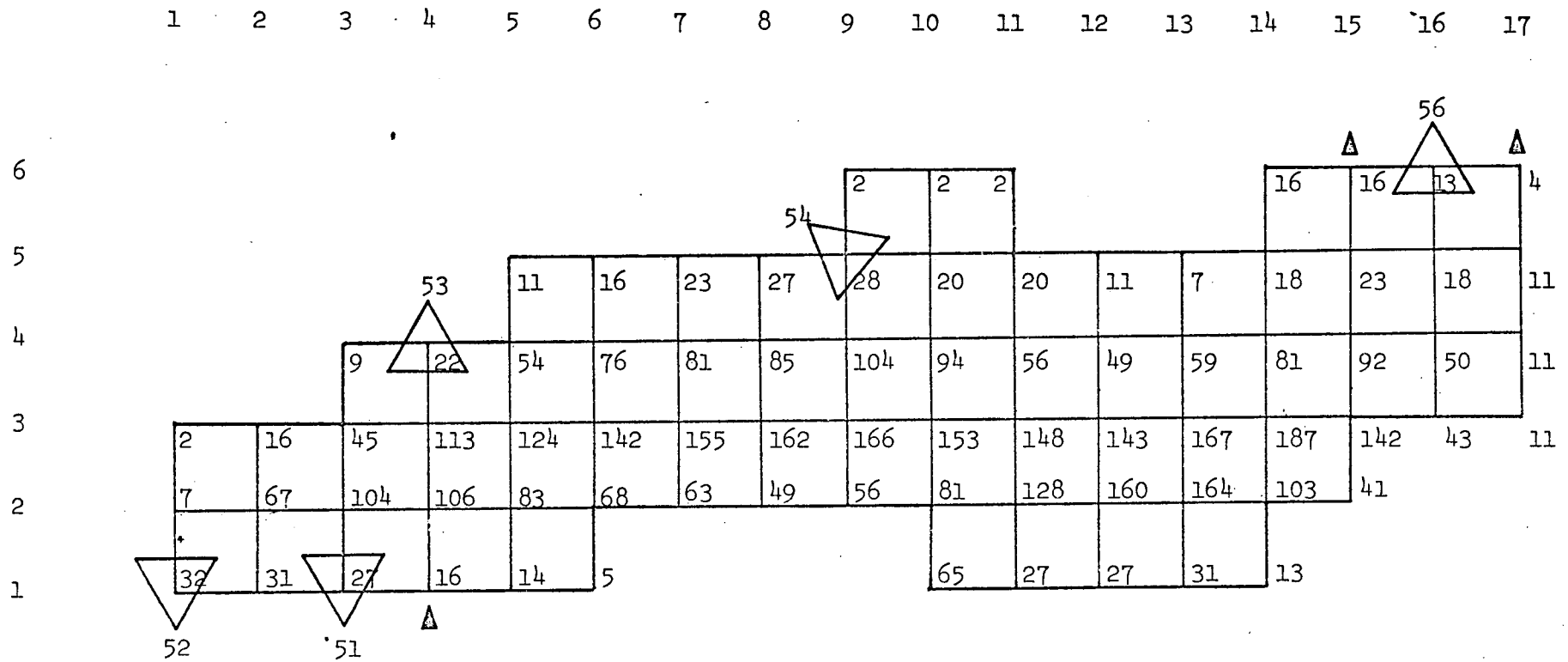


LEGEND

-  H calculation
-  U & V calculation
-  direction of flow

Grid System: 17.7 x 17.7 kilometers
Uniform Depth: 60.96 meters

Figure 3 Simplified Rectangular Model



LEGEND



direction of flow

51 water level gauging station 51 (Canadian System)

depth in meter at the grid point

Grid System: 17.7 x 17.7 kilometers

Figure 4 Real Numerical Model of Lake Ontario

FIGURE 5

CHEZY'S COEFFICIENT
"C"

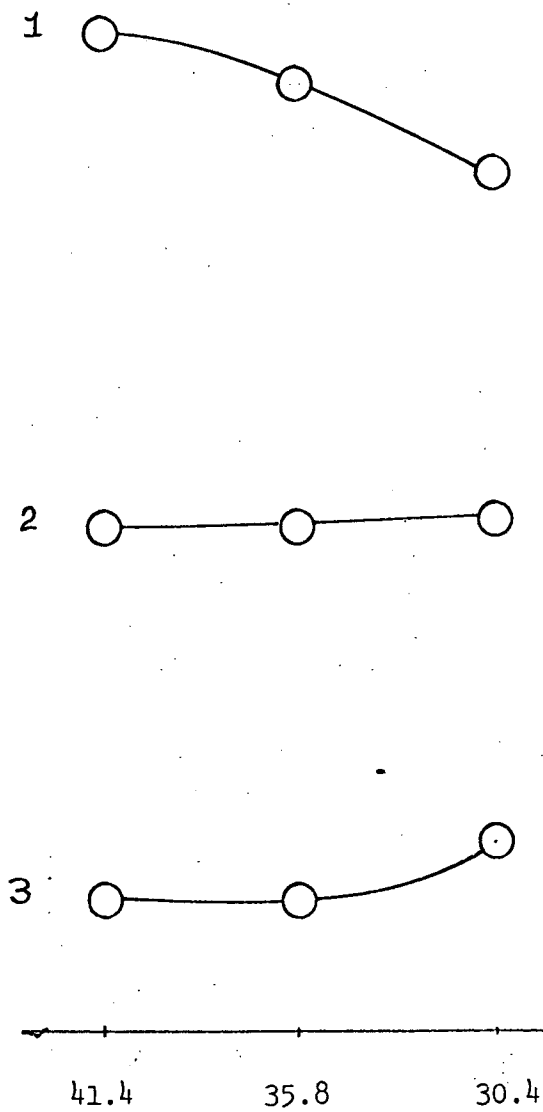
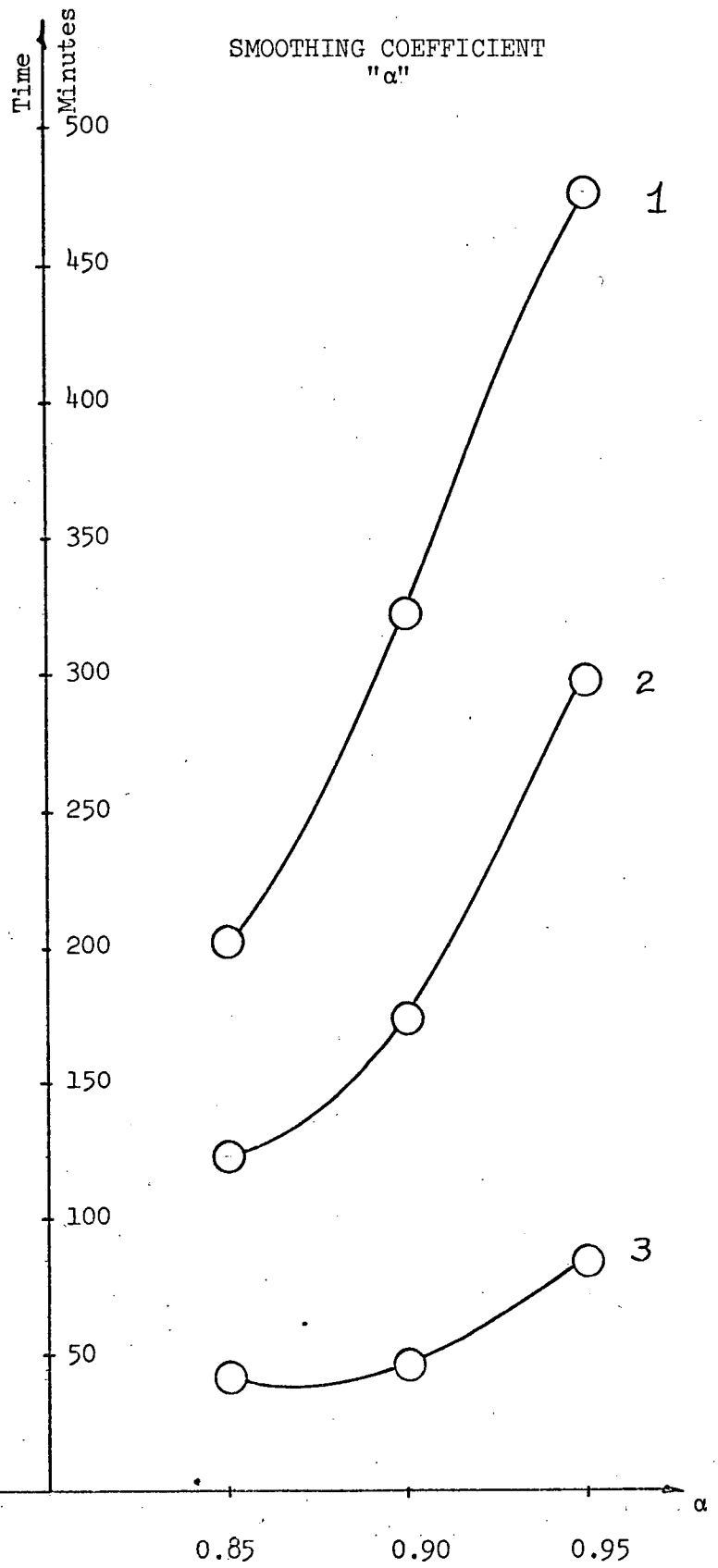


FIGURE 6

SMOOTHING COEFFICIENT
"α"



CURVE 1: MAXIMUM
CURVE 2: MEAN
CURVE 3: MINIMUM

FIGURE 7
TIME STEP
" Δt "

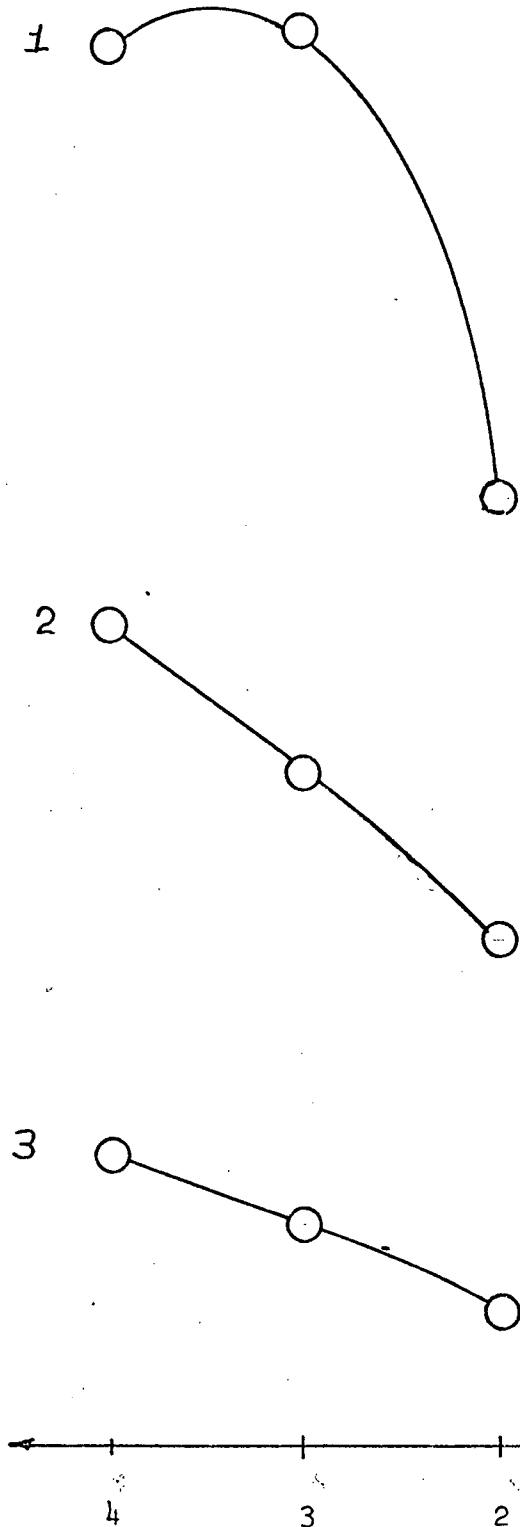
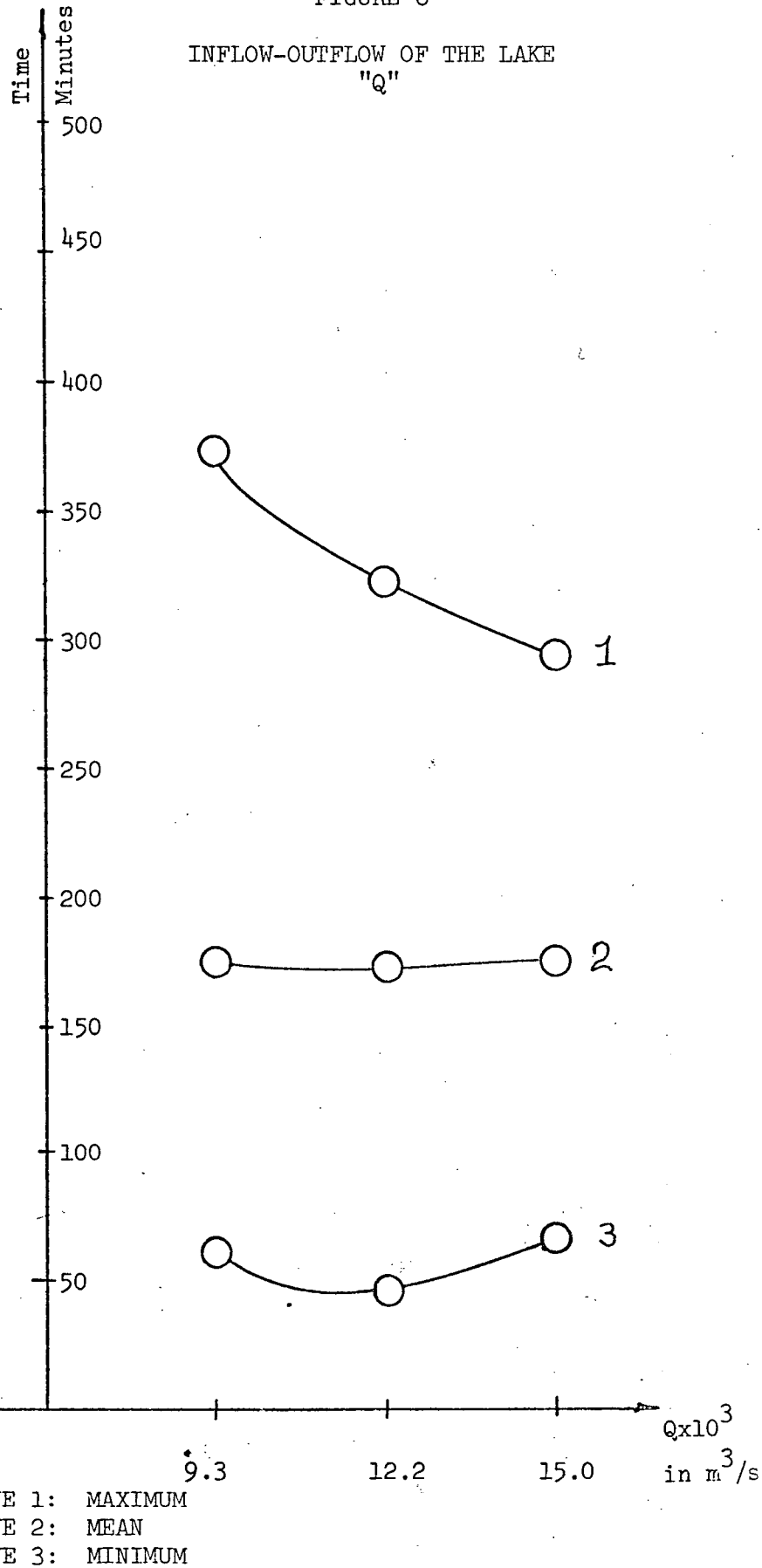
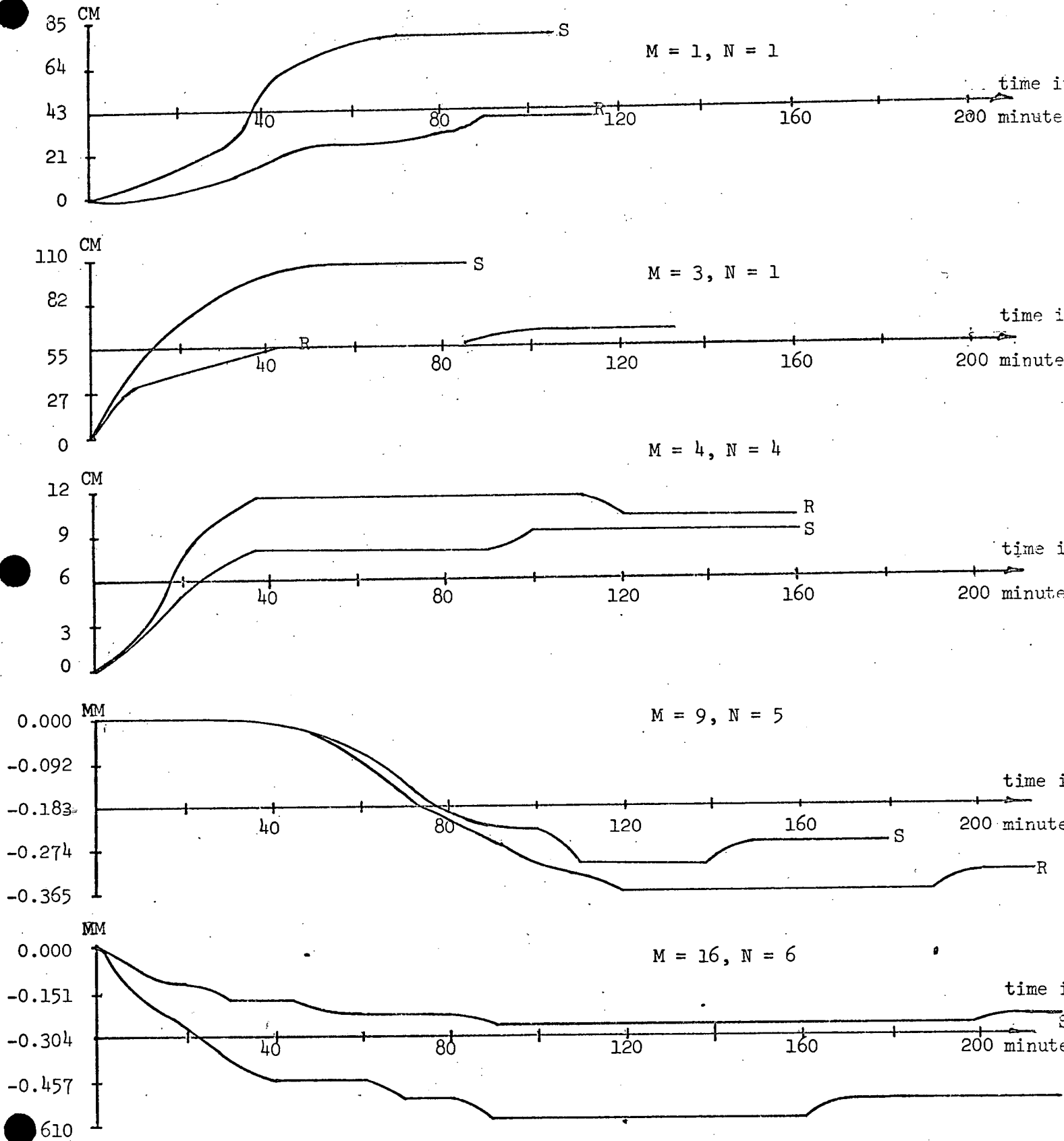


FIGURE 8
INFLOW-OUTFLOW OF THE LAKE
" Q "





R = REAL
S = SIMPLIFIED

Figure 9
Comparison Between the Simplified
and the Real Model

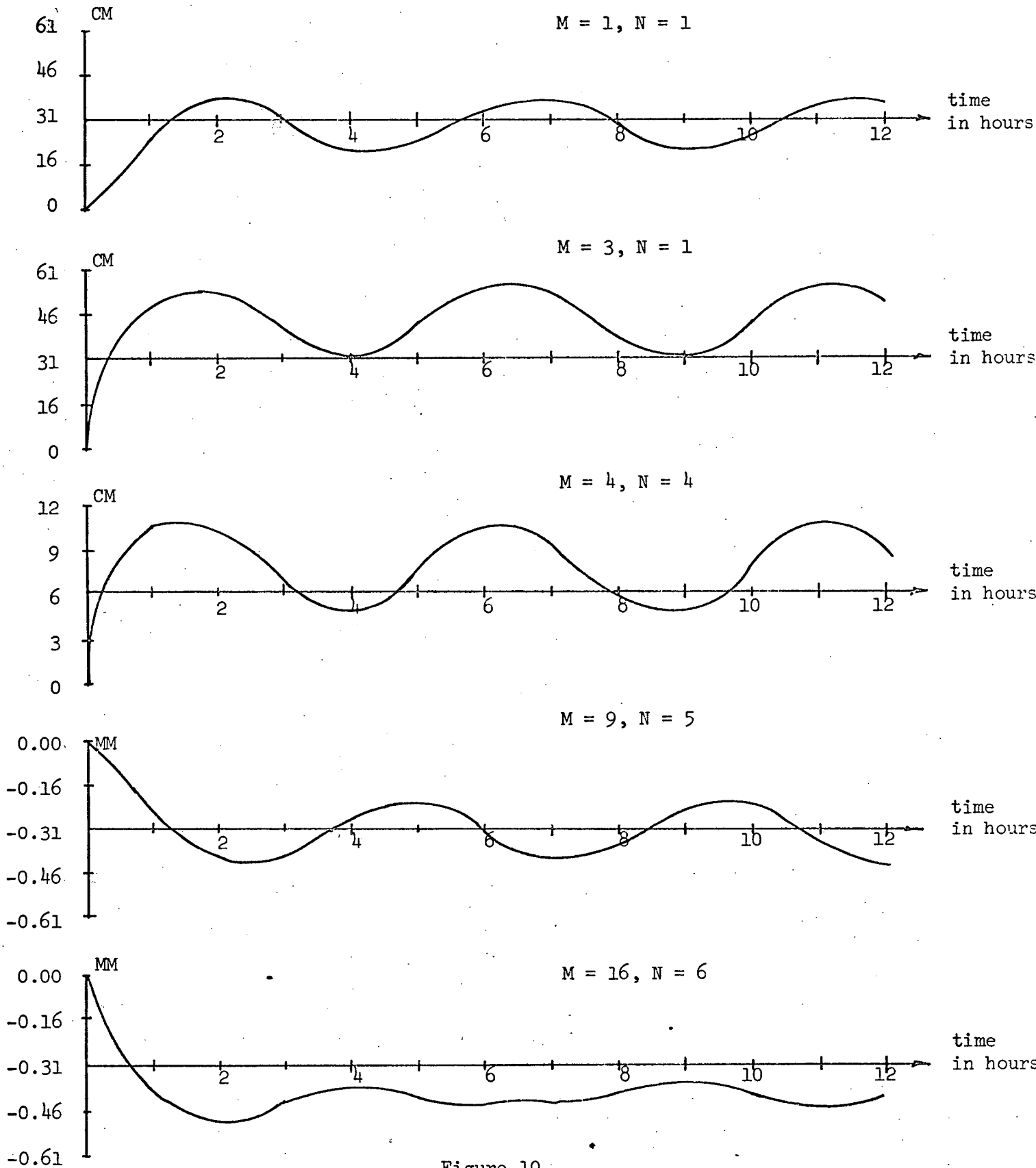
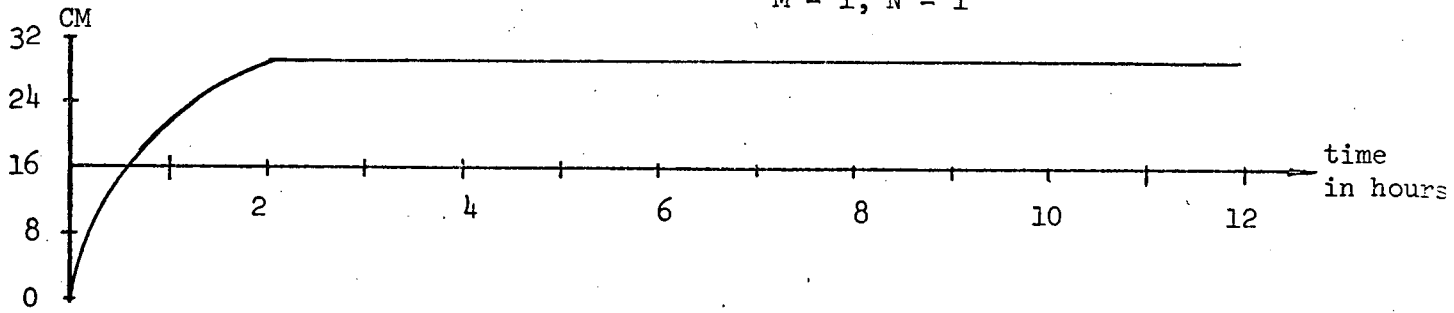
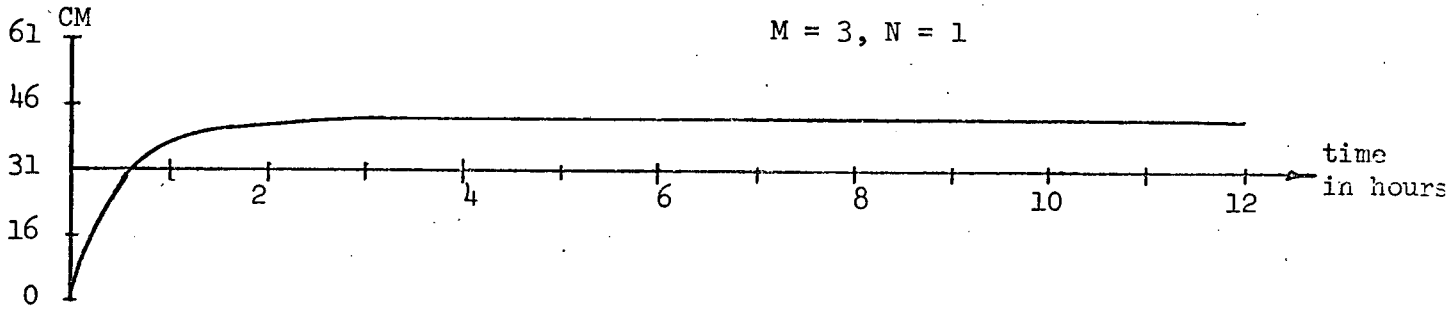


Figure 10
Response of the Model
to the Input Sine Function

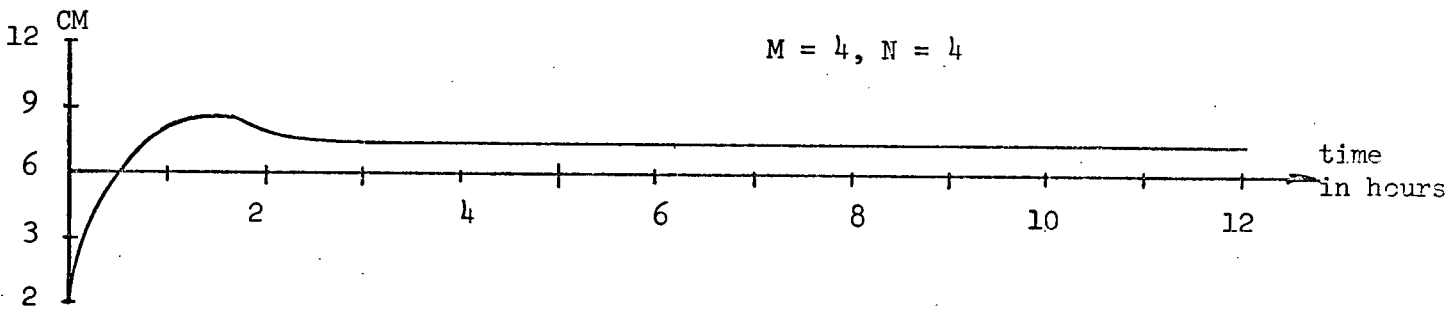
$M = 1, N = 1$



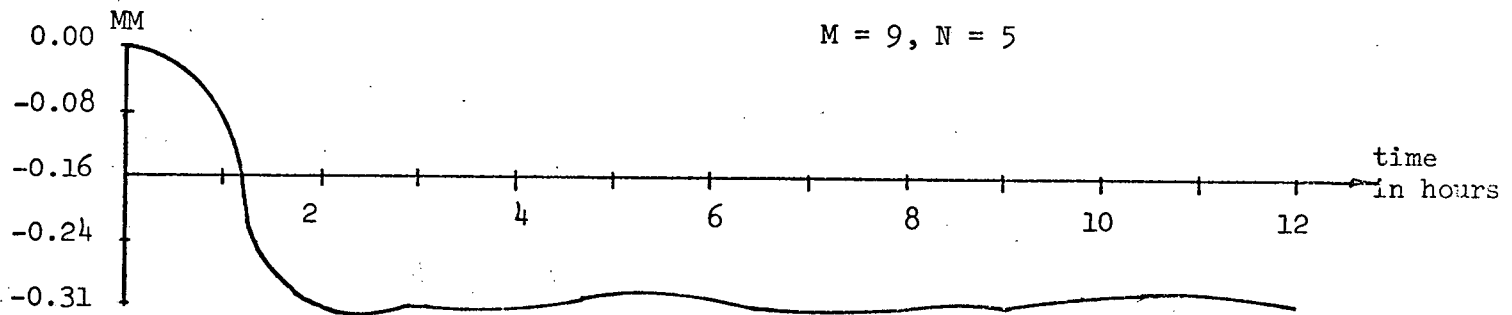
$M = 3, N = 1$



$M = 4, N = 4$



$M = 9, N = 5$



$M = 16, N = 6$

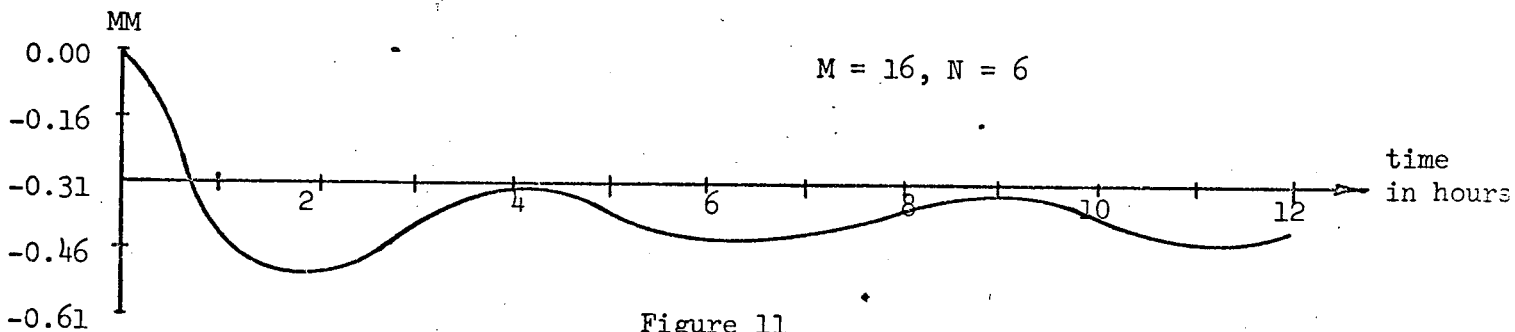


Figure 11
Response of the Model
To the Output Sine Function

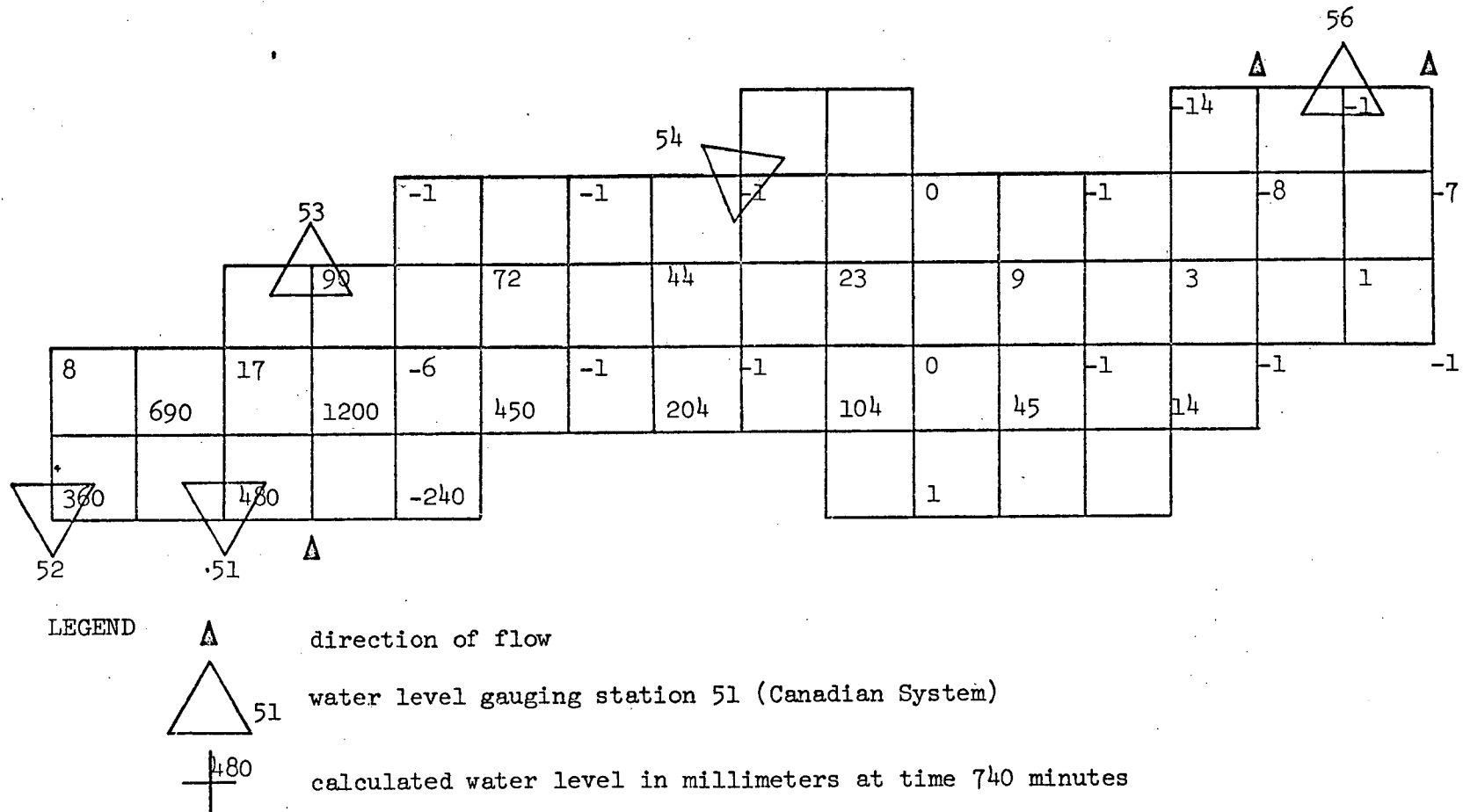


Figure 12 Calculated Water Level with Sine Function applied to the Niagara

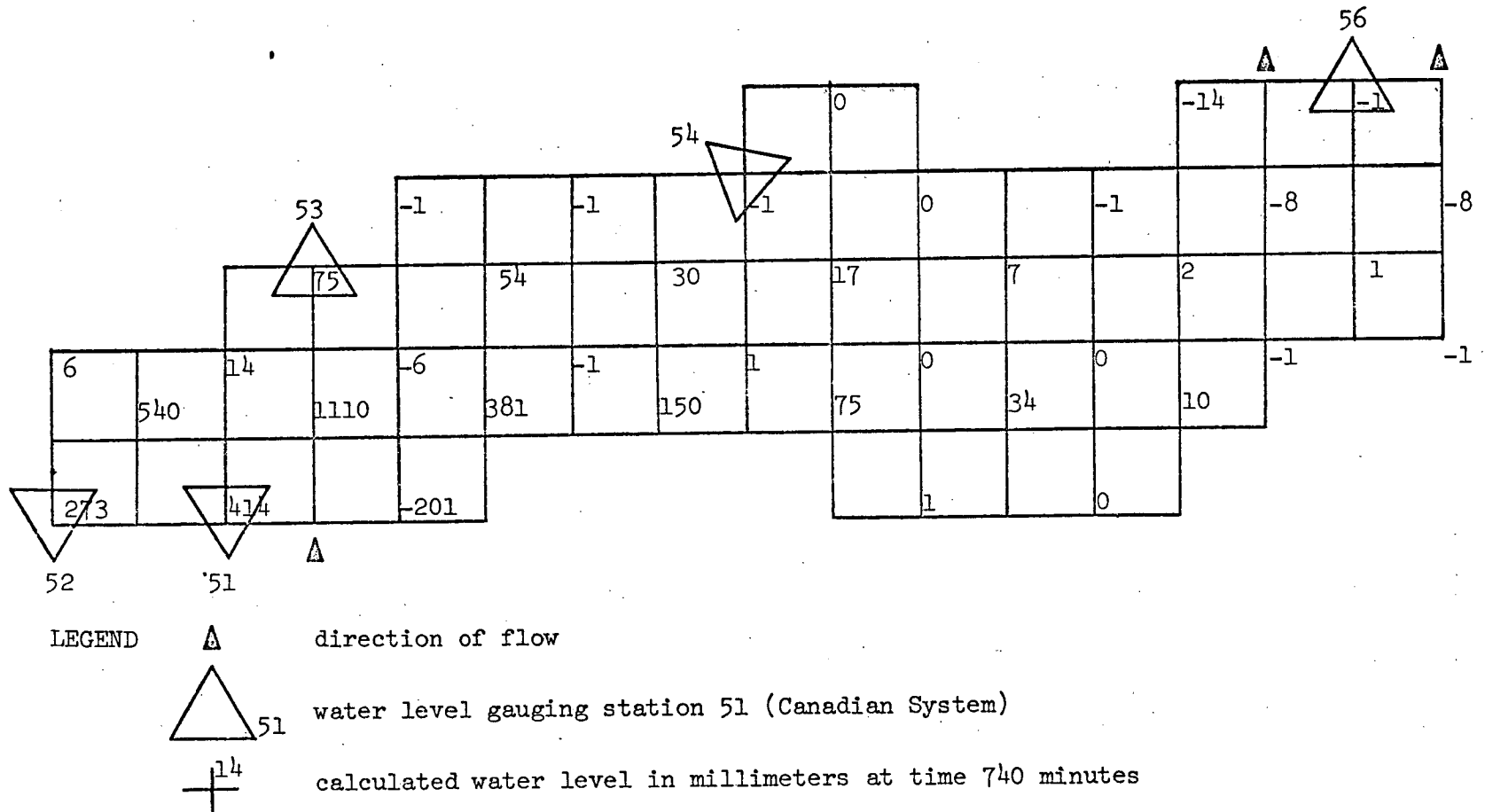


Figure 13 Calculated Water Level with Sine Function applied to the St. Lawrence

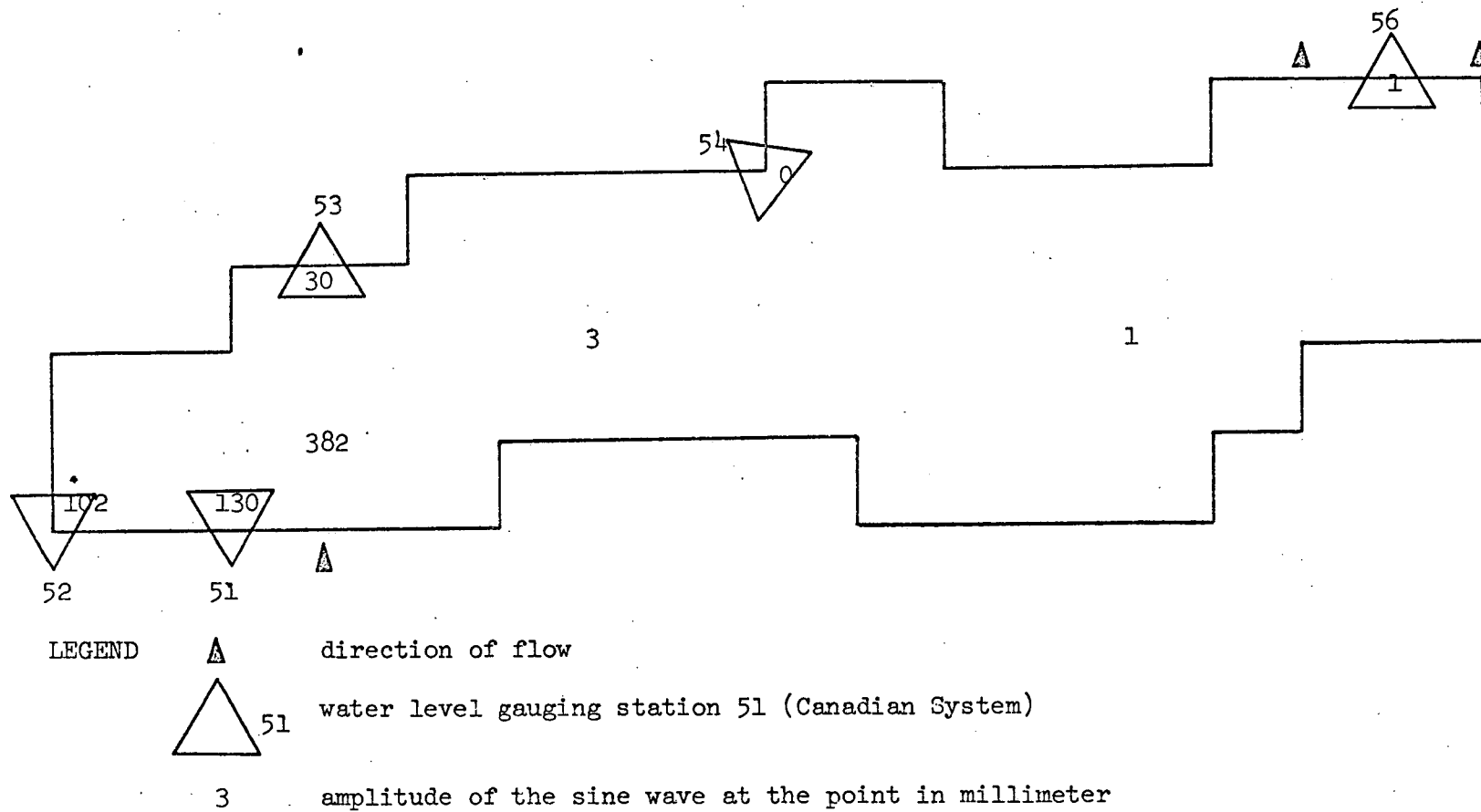


Figure 14 Amplitude of the Sine Wave
for Particular Points in Lake Ontario
Sine Function applied to the Niagara

Table 1

Discharge Values Used in the Model
in Cubic Meters/Second

	Q0	Q1	QCTE
St. Lawrence River	6866.8	1175.1	7135.7
Niagara River	6532.1	2325.7	6294.3

frequency $\omega = 0.000362844$ radian/second

Table 2

Amplitude of the Sine Wave
in Millimeters

Sine Function Applied to the Input

M-N	MAXIMUM	MEAN	AMPLITUDE
1-1	380	278	102
3-1	568	438	130
4-2	1606	1224	382
4-4	111	81	30
7-3	4	1	3
9-5	0	0	0
13-3	1	0	1
15-5	8	7	1
16-6	1	0	1
17-5	1	0	1

Printed in U.S.A.